Figure S1.

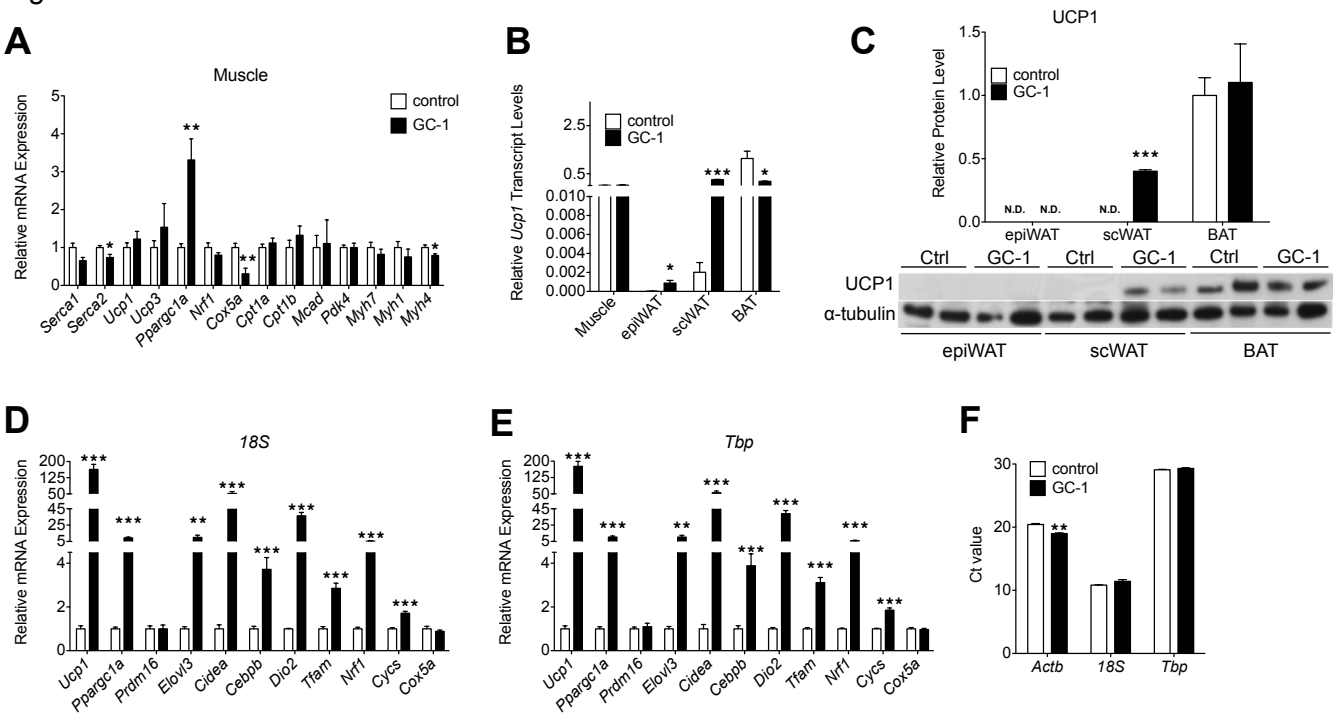
A
Muscle
control
GC-1
Relative mRNA Expression
Serca1
Serca2
Ucp1
Ucp3
Ppargc1a
Nrf1
Cox5a
Cpt1a
Cpt1b
Mcad
Pdk4
Myh7
Myh1
Myh4
B
control
GC-1
Relative Ucp1 Transcript Levels
Muscle
epiWAT
scWAT
BAT
C
UCP1
control
GC-1
Relative Protein Level
N.D.
epiWAT
scWAT
BAT
Ctrl
GC-1
UCP1
α-tubulin
epiWAT
scWAT
BAT
D
18S
Relative mRNA Expression
Ucp1
Ppargc1a
Prdm16
Elovl3
Cidea
Cebpb
Dio2
Tfam
Nrf1
Cycs
Cox5a
E
Tbp
Relative mRNA Expression
Ucp1
Ppargc1a
Prdm16
Elovl3
Cidea
Cebpb
Dio2
Tfam
Nrf1
Cycs
Cox5a
F
control
GC-1
Ct value
Actb
18S
Tbp

Figure S2.

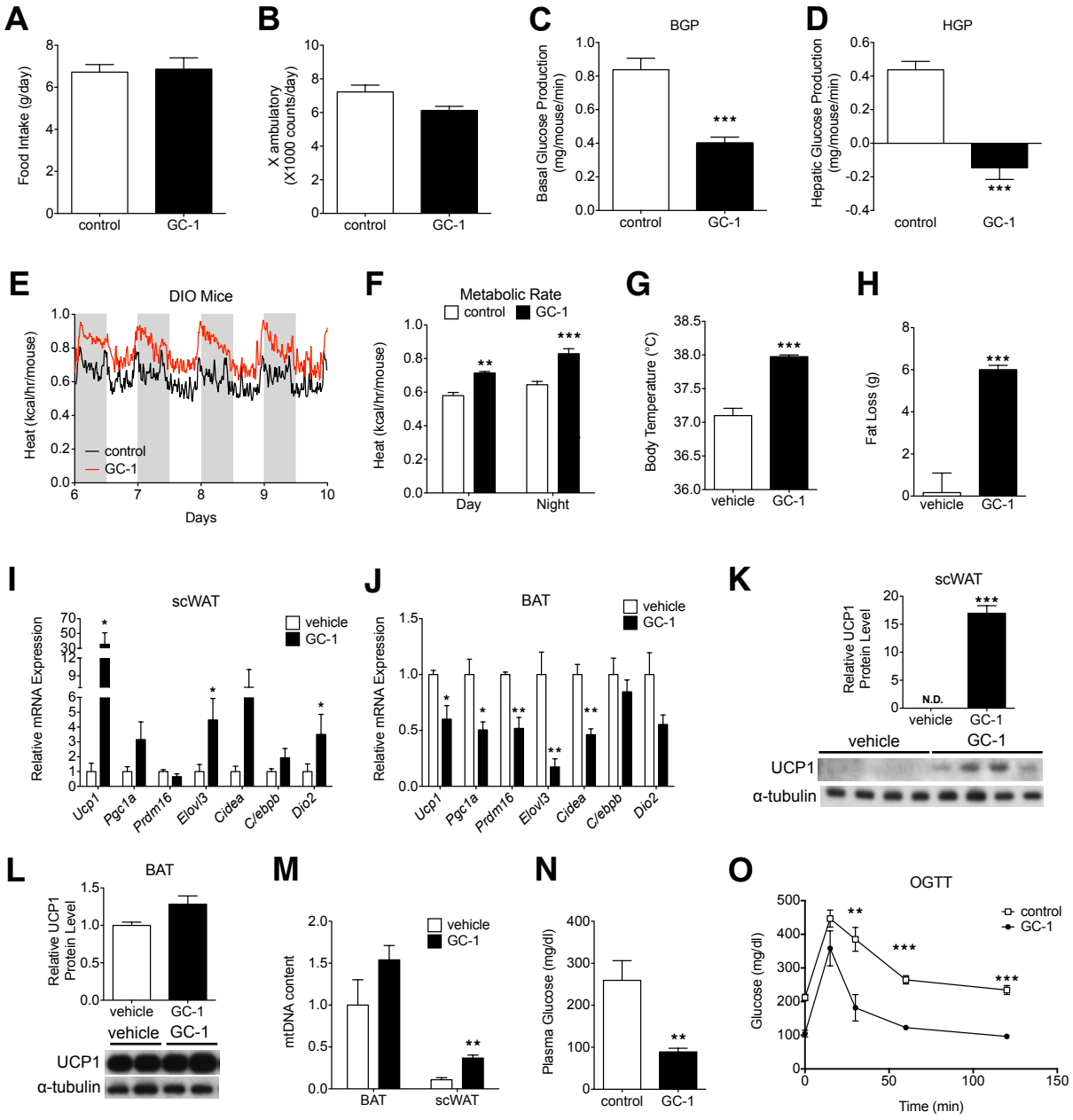
A
Food Intake (g/day)
control
GC-1
B
X ambulatory (X1000 counts/day)
C
BGP
Basal Glucose Production (mg/mouse/min)
D
HGP
Hepatic Glucose Production (mg/mouse/min)
E
DIO Mice
Heat (kcal/hr/mouse)
Days
F
Metabolic Rate
Day
Night
G
Body Temperature (°C)
vehicle
H
Fat Loss (g)
I
scWAT
Relative mRNA Expression
Ucp1
Pgc1a
Prdm16
Elovl3
Cidea
C/ebpb
Dio2
J
BAT
K
Relative UCP1 Protein Level
N.D.
UCP1
α-tubulin
L
M
mtDNA content
N
Plasma Glucose (mg/dl)
O
OGTT
Glucose (mg/dl)
Time (min)

Figure S3.

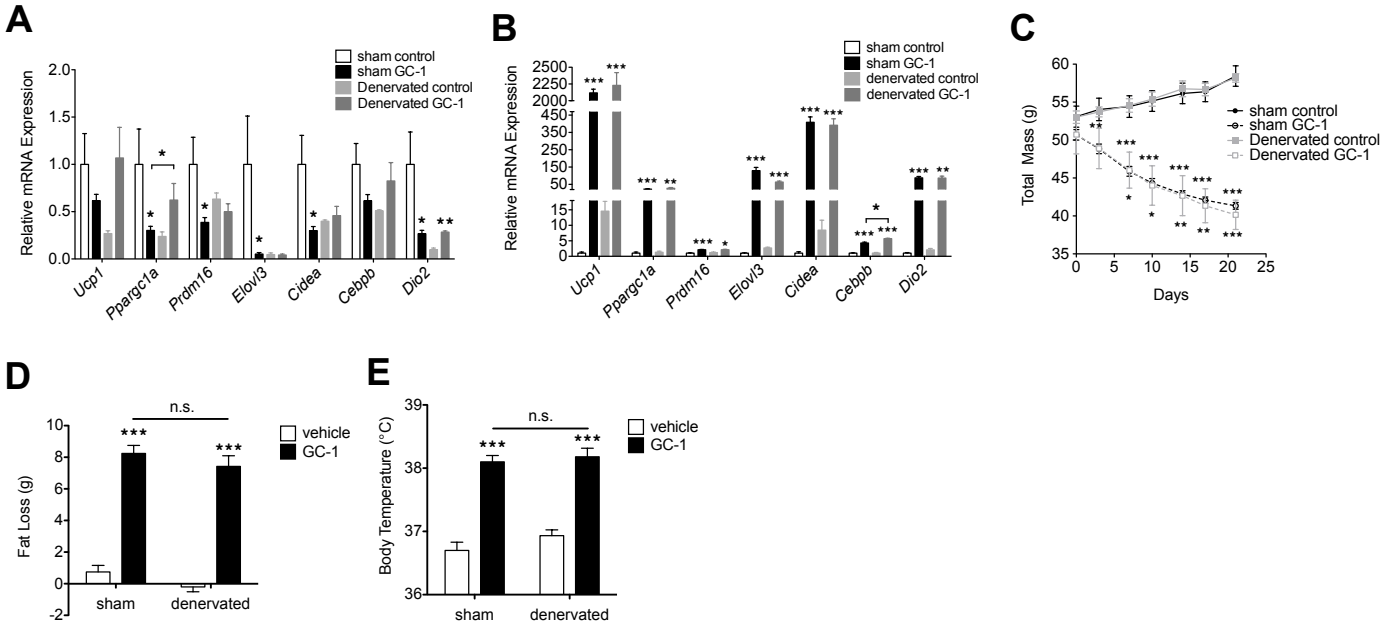
A
Relative mRNA Expression
sham control
sham GC-1
Denervated control
Denervated GC-1
Ucp1
Ppargc1a
Prdm16
Elovl3
Cidea
Cebpb
Dio2
B
Relative mRNA Expression
sham control
sham GC-1
denervated control
denervated GC-1
C
Total Mass (g)
Days
sham control
sham GC-1
Denervated control
Denervated GC-1
D
Fat Loss (g)
n.s.
vehicle
GC-1
sham
denervated
E
Body Temperature (°C)
n.s.
vehicle
GC-1
sham
denervated

Figure S4.

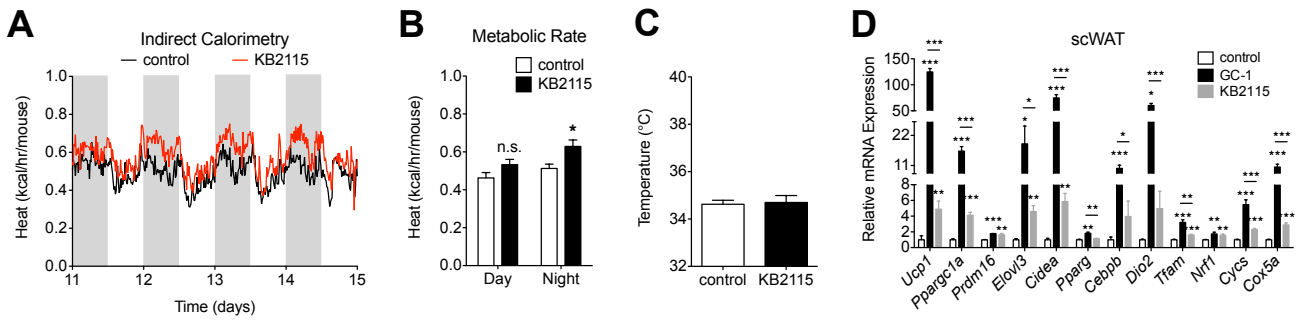
A
Indirect Calorimetry
control
KB2115
Heat (kcal/hr/mouse)
Time (days)
B
Metabolic Rate
control
KB2115
n.s.
*
Heat (kcal/hr/mouse)
Day
Night
C
Temperature (°C)
control
KB2115
D
scWAT
control
GC-1
KB2115
Relative mRNA Expression
Ucp1
Ppargc1a
Prdm16
Elovl3
Cidea
Pparg
Cebpb
Dio2
Tfam
Nrf1
Cycs
Cox5a

Supplemental Figure Legends

Figure S1. GC-1 induces thermogenic markers in WAT, related to Figure 1.
(A) Thermogenic gene expression in gastrocnemius muscle of GC-1-treated and control mice (n = 4 – 5).
(B) Relative *Ucp1* transcript levels in muscle, epiWAT, scWAT, and BAT (n = 4 – 5). Values were normalized to β-actin.
(C) UCP1 protein quantification and immunoblot of epiWAT, scWAT and BAT of GC-1 treated and control mice, α-tubulin was used as a loading control (n = 4 – 5). N.D. not detectable.
(D and E) Thermogenic gene expression in scWAT normalized with endogeneous controls 18S (D) and Tbp (E).
(F) Ct value of endogeneous controls Actb, 18S and Tbp in scWAT of control and GC-1 treated mice.
Data are mean ± s.e.m. *P < 0.05, **P < 0.01, ***P < 0.001. N.D. not detectable.

Figure S2. WAT browning coincides with supraphysiological thermogenesis *in vivo*, related to Figure 2.
(A and B) Food intake (A) and ambulatory activity (B) of GC-1 treated and control ob/ob mice was averaged over 3 days.
(C – D) Basal glucose production rate (C) and hepatic glucose production rate (D) discerned from hyperinsulinemic-euglycemic clamp experiment of GC-1-treated and control ob/ob mice.
(E – P) DIO C57Bl6 were treated with GC-1 (4.8 mg/kg-diet) or control diet for 14 days (n = 4). Metabolic rate (E and F), final body temperature (G) and fat loss (H) of DIO mice with or without GC-1 treatment.
(I and J) Thermogenic gene expression in scWAT (I) and BAT (J).
(K and L) UCP1 protein expression in scWAT (K) and BAT (L), α-tubulin was used as a loading control.
(M) Mitochondrial DNA content in BAT and scWAT.
(N and O) Fasting glucose levels (O) and glucose tolerance (P) of DIO mice after 14 days of GC-1 administration.
Data are mean ± s.e.m. *P < 0.05, **P < 0.01, ***P < 0.001. N.D. not detectable.

Figure S3. GC-1-mediated thermogenesis is independent of BAT activity and dependent on Ucp1, related to Figure 3.
(A – C) Male obob mice were subject to either BAT denervation surgery or sham (n = 6 per sham; n = 3 per BAT denervated group). Thermogenic gene expression in BAT (A) and scWAT (B) and weight loss (C) in BAT-denervated and sham-treated mice.
(D and E) Male DIO mice were subject to either BAT denervation surgery or a sham operation (n = 4 per sham group; n = 6 per BAT denervated group). Fat loss relative to initial fat mass (C) and body temperature (D) of BAT-denervated and sham treated DIO mice after 14 days of GC-1 or vehicle treatment.
Data are given as mean ± s.e.m. *P < 0.05, **P < 0.01, ***P < 0.001.

Figure S4. WAT browning and thermogenesis is not a common effect of all TR agonists, related to Figure 4.
(A – D) Male ob/ob mice were administered KB2115 admixed in chow diet (3 mg/kg-diet) or control diet for 21 days (n = 5 – 6). Metabolic rate (A and B), body temperature (C) and thermogenic gene expression in scWAT (D) of KB2115 or control mice.
To facilitate comparison with GC-1 treatment, the same scales are used as in Figs. 1 and 2 and GC-1 data from Fig. 1B is re-plotted in (C). Data are given as mean ± s.e.m. *P < 0.05, **P < 0.01, ***P < 0.001.

Supplemental Experimental Procedures

Hyperinsulinemic-Euglycemic Clamp

Hyperinsulinemic-euglycemic clamps were performed at the Mouse Metabolism Core at Baylor College of Medicine. Prior to the clamp, a catheter was inserted into the right internal jugular vein. After recovery, mice were administered GC-1 admixed in diet for 10-12 days. On the day of the experiment, conscious, overnight-fasted mice received a primed intravenous infusion of ^{3}H-glucose (10 µCi) to measure glucose turnover. The hyperinsulinemic-euglycemic clamp was performed with continuous infusion of insulin (12 mU/kg/min) and variable infusion of glucose to maintain euglycemia. Blood samples were collected every 10 min to measure glucose concentrations. Glucose disposal rate was calculated by adding the whole body glucose flux during clamp condition to the glucose infusion rate during the same time period. Glucose flux was calculated from specific activity during that period. Tissue-specific uptake was performed using ^{14}C-deoxyglucose (10 µCi) 45 min before the end of the clamp experiment.

PET/CT Imaging
^{18}F-deoxyglucose (^{18}F-FDG) (200 µCi) was administered to mice that had received GC-1 via intraperitoneal injection for 14 days. Animals were imaged 1 h after FDG injection at the HMRI preclinical imaging core. microPET/CT imaging was performed using Siemens Inveon dedicated PET and Siemens Inveon multimodality system in docked mode. Anesthetized animals were first subjected to a whole-body CT scan and then to a static ^{18}F PET scan. CT and PET images were aligned and reconstructed with Inveon Research Workplace software (Siemens).

Oxygen Consumption Rate Analysis
Oxygen consumption rates were determined in mouse adipose tissue and subcutaneous adipocytes using a modified protocol (Yehuda-Shnaidman et al., 2010). Inguinal fat depots were extracted from mice and rinsed in XF-DMEM (Seahorse Bioscience) containing 2.5 mM glucose and 1 mM sodium pyruvate. Adipose tissues were cut into small pieces (~10 mg), rinsed in XF-DMEM media, and immobilized in XF24-well Islet Flux plate (Seahorse Bioscience). Oxygen consumption rate was measured using an Extracellular Flux XF24 analyzer (Seahorse Bioscience) at 37°C. The XF24 Analyzer mixed the media in each well for 2 min before measurements to allow oxygen partial pressure to equilibrate. Basal OCR was measured simultaneously in all wells four times. Tissue replicates from different mice were analyzed in independent experiments and results were normalized to tissue weight. Despite repeated efforts, we were unable to measure leak respiration, presumably due to poor penetrance of oligomycin into the tissue. For subcutaneous white adipocytes, preadipocytes were plated in a 24-well XF24 cell culture microplate followed by adipocyte differentiation. On the day of the experiment the cells were washed with XF-DMEM and 500 µl of XF-DMEM was added to each well, and the cells were incubated at 37°C without CO_2 for 1 h before the assay. Leak respiration was measured after the addition of oligomycin (2 µg/ml), an ATP synthase inhibitor. Maximal respiration was measured after the addition of 1.5 µM FCCP (carbonyl cyanide p-trifluoromethoxyphenylhydrazone).

Metabolic Phenotyping
Glucose tolerance tests were performed on mice fasted for 6 h and administered a bolus of glucose (2 g/kg BW) via oral gavage. Blood glucose concentrations were measured at indicated intervals with a standard glucometer (OneTouch). Body composition analysis was performed using noninvasive quantitative NMR (EchoMRI).

Indirect Calorimetry
Metabolic rate, RER, food intake and ambulatory activity were evaluated by using a Comprehensive Laboratory Animal Monitoring System (Columbus Instruments). Mice were individually housed in metabolic cages with food and water *ad libitum* and allowed to acclimate for 48 h prior to experimentation. Mice were fed chow with or without GC-1 admixed. CO_2 and O_2 levels were measured at 15 min intervals. Metabolic rate, food intake and ambulatory activity were averaged over 72-h.

Acute Cold Challenge.
Mice were individually housed with food and water *ad libitum* and challenged with acute cold at 4°C. Core body temperature was measured prior to cold exposure and at time intervals indicated using a digital thermometer with RET-3 rectal probe for mice.

RNA Extraction and Real-Time qPCR
Total RNA was extracted and isolated using QIAzol and RNeasy Mini Kit (Qiagen). First strand cDNA was transcribed from total RNA using SuperScript VILO master mix (Invitrogen). TaqMan real-time PCR reactions were performed on a LightCycler 480 Real-Time PCR system (Roche), and relative mRNA levels were calculated by the comparative Ct method using beta-actin as internal control. TaqMan primer/probe sets were supplied by Applied Biosystems. Assay IDs are available upon request. To ensure that the large changes in expression levels observed in scWAT were not simply due to changes in Ct values of the gene chosen for normalization, expression was also calculated using alternate genes, 18S and TBP, for normalization and we assessed for changes in Ct values that resulted from GC-1 treatment (Figure S1D – S1F).

Mitochondrial DNA Content
RNA-free genomic DNA was isolated from epididymal WAT, subcutaneous WAT and BAT using DNeasy Blood and Tissue Kit (Qiagen). Real-time quantitative qPCR analysis was used to measure the genomic level of mitochondrial NADH dehydrogenase subunit 1 (ND1), which was normalized to nuclear 18S ribosomal DNA.

Histology
Adipose tissues were fixed in 10% buffered formalin, paraffin-embedded, and sectioned (6 μm) prior to hematoxylin and eosin (H&E) and UCP1 (Abcam, ab10683) immunohistochemistry staining. Signal was detected using Vector ABC Elite kit and counterstain was performed with hematoxylin.

Immunofluorescence
Immunofluorescence was performed on stromal vascular cells differentiated in the presence or absence of GC-1. Briefly, cells were fixed in 4% formaldehyde in PBS, quenched with 0.1 M ammonium chloride for 10 min, and permeabilized with 0.1% Triton X-100 for 10 min. Primary antibody was added overnight at 4°C prior to 1 hr of secondary antibody (AlexaFluor-647; Invitrogen). Antibody incubations were performed in 2% BSA/0.01% saponin PBS solution. DAPI was used to visualize the nucleus. The primary antibodies used were rabbit anti-UCP1 (Abcam, ab10683).

Adipose Tissue Citrate Synthase Activity
BAT, inguinal WAT, and epididymal WAT were homogenized in CelLytic MT lysis reagent (Sigma) containing a cocktail of protease inhibitors (Roche). Lysates were centrifuged to remove cell debris and lipids. Protein concentration was determined using a NanoDrop spectrophotometer (Thermo Fisher Scientific Inc.). Citrate synthase activity in the protein lysates was measured with a kit (Sigma) following the manufacturer's protocol.

Catecholamines
Norepinephrine content in BAT and inguinal WAT were determined using a commercially available ELISA kit and according to manufacturer's instructions (Rocky Mountain Diagnostics). Tissues were homogenized in buffer containing 1 mM EDTA and 4 mM $Na_2S_2O_5$ to stabilize and prevent degradation of norepinephrine.

Western Blot
Adipose tissue was homogenized in tissue extraction reagent (Invitrogen) containing a cocktail of protease inhibitors (Roche). Equivalent amounts of total protein were separated by SDS-PAGE, transferred to polyvinylidene difluoride membranes and probed with antibodies against UCP1 (Abcam, ab10683) and α tubulin (Abcam, ab7291), and with conjugated-HRP anti-rabbit (Santa Cruz Biotechnology, sc sc-2004) and anti-mouse antibodies (Santa Cruz Biotechnology, sc-2005). Blots were visualized by autoradiography using Amersham ECL Western Blotting Detection Regents (GE Healthcare).